

## Cu (II) Ion-Selective Electrode Based on Mixed Silver-Copper Sulfide: Phase Structure and Electrochemical Properties

Slobodan Brinić<sup>1,\*</sup>, Marijo Buzuk<sup>2</sup>, Marija Bralić<sup>2</sup>, Maša Buljac<sup>2</sup>, Dražan Jozić<sup>3</sup>

<sup>1</sup>Department of General and Inorganic Chemistry, Faculty of Chemistry and Technology, Teslina 10/V, 21000 Split, Croatia

<sup>2</sup>Department of Environmental Chemistry, Faculty of Chemistry and Technology, Teslina 10/V, 21000 Split, Croatia

<sup>3</sup>Department Inorganic Technology, Faculty of Chemistry and Technology, Teslina 10/V, 21000 Split, Croatia

\*E-mail: [brinic@ktf-split.hr](mailto:brinic@ktf-split.hr)

Received: 27 April 2012 / Accepted: 18 May 2012 / Published: 1 June 2012

---

Mixed silver-copper sulfide precipitates have been prepared at different mole ratio between metal ions ( $\text{Ag}^+$ ;  $\text{Cu}^{2+}$ ) toward sulfide and tested for their suitability as  $\text{Cu}^{2+}$  ion-selective membranes (ISE). Characterization of prepared precipitates by X-ray diffractometry (XRD) showed that all three powders consisted of ternary sulfides while in two powders metallic silver was founded. Origin of different electrical resistance of the prepared materials is discussed. Potentiometric study in  $\text{KNO}_3$  together with spectrophotometric measurements in ethylenediamine solution showed that differences in detection limits can be attributed to the membranes solubility. Also, electrochemical impedance spectroscopy (EIS) study revealed contribution of the hysteresis effect on the high detection limit due to the contamination of the electrode surface by primary ions. Changes of electrical resistance of the electrode ( $R_{\text{memb}}$ ), related to the variation of the charge transfer resistance ( $R_{\text{ct}}$ ) and perturbation in the diffusion layer, as possible explanation for sub-Nernstian response are also discussed. Some potentiometric characteristics as: standard potential, calibration curves, detection limits, pH ranges and time responses of the electrodes are resumed and discussed. These findings offer a novel approach for understanding of response mechanism of electrodes based on the mixed metal sulfide.

---

**Keywords:** silver-copper sulfides, impedance spectroscopy, ion-selective electrodes, X-ray diffractometry

### 1. INTRODUCTION

Ion-selective electrodes (ISEs) are established tools that are capable of determining the activities of many analytes. Since Ross and Frant introduced the use of metal sulfide membranes for

ion-selective electrodes as sensors for copper (II), cadmium(II) and lead(II) ions, many authors have published different methods for the preparation of  $\text{Cu}^{2+}$  ion-selective electrodes. The characteristic of these electrodes will depend of two main aspects, i.e. the way of preparing the electroactive material and the way in which this material is applied to construct the actual electrode [1, 2].

Although, different materials for preparation of copper-selective electrode were used (chalcogenide glasses [3-5] and ionophores [6-11]) most common commercial copper ISE are those based on mixed metal sulfides, mainly silver-copper sulfides. Excellent review of solid state electrodes, with emphasis on electrodes based on simultaneously precipitated silver-copper sulfides (mainly consisted of the ternary compound jalpaite- $\text{Ag}_3\text{CuS}_2$ ) with Nernstian response to  $\text{Cu}^{2+}$  ions was presented by Gulens [12]. High detection limit of these electrodes were attributed to membrane oxidation [13], dissolution of the electrode and contamination of diffusion layer [14, 15] or to the contamination of electrode surface, in the presence of halide ions, by formation of amorphous sulphur [16]. Also, an EIS (electrochemical impedance spectroscopy) study of response mechanism of the jalpaite, performed by de Marco [17], revealed that response of the jalpaite electrode is underpinned by the  $\text{Cu}^{2+}/\text{Cu}^+$  charge transfer layer at the membrane/electrolyte interface.

It is known that in the process of co-precipitation of the mixed silver-copper sulfides, in addition to jalpaite, other ternary compounds can be formed. Presence of such ternary compounds, in the electroactive material, can make interpretation and understanding of the electrode response more complex [2]. However, limited information are available regarding electrodes for determination of  $\text{Cu}^{2+}$  based on the other silver-copper compounds which are prepared by simultaneously precipitations of mixed metal salts with  $\text{Na}_2\text{S}$  at different mole ratio. Electrochemical properties and limitation in potentiometric characteristics, observed at these electrodes, can be helpful for understanding response mechanism and origin of mentioned limitations. In this study,  $\text{Cu}^{2+}$  ion-selective electrodes (ISE) based on the different electroactive materials, prepared by co-precipitation of the mixed metals ions ( $\text{Cu}^{2+}$ ,  $\text{Ag}^+$ ) and  $\text{S}^{2-}$  (from  $\text{Na}_2\text{S}$ ) at different mole ratio (1:0.5; 1:1; 1:1.8), were fabricated and characterized by spectrophotometry, potentiometry and EIS techniques. The phase composition has been determined by using X-Ray diffraction (XRD) on powder sample. Using above techniques, phenomena responsible for non-Nernstian response, narrowed linear range and high detection limit are explained.

## 2. EXPERIMENTAL

### 2.1. Reagents

All chemical were of analytical reagent grade. All solutions were prepared with doubly distilled water.

Standard  $\text{Cu}^{2+}$  solution (0.1 M) was prepared in a calibrated glass flask from copper(II) nitrate trihydrate (Kemika Zagreb, Croatia) diluted in doubly distilled water. The  $\text{Cu}^{2+}$  solution was titrated by a standardized 0.01 M EDTA solution. EDTA was obtained from Sigma Aldrich (St. Louis, USA). Common stock solution was used for the preparation of 0.1 and 0.01 M solutions. The sodium sulfide

solution was prepared by dissolving a certain amount of Na<sub>2</sub>S (Kemika Zagreb, Croatia) in double distilled water. Concentration of such solution was determined with lead nitrate standard solution.

Silver nitrate solution (0.1 M) was prepared from silver nitrate obtained from Kemika (Zagreb, Croatia). The silver nitrate was standardized with 0.1 M sodium chloride.

Sodium hydroxide and hydrochloric acid were provided by Kemika (Zagreb, Croatia).

## 2.2. Preparation of electrode materials

For the preparation of electroactive materials by simultaneous precipitation of copper(II) sulfide and silver(I) sulfide three reagents have been used: copper(II) nitrate (Cu(NO)<sub>3</sub> × 3H<sub>2</sub>O), silver nitrate (AgNO<sub>3</sub>) and sodium sulfide (Na<sub>2</sub>S × 9H<sub>2</sub>O). The procedure was adopted from Czban and Rechnitzv [18], and modified in respect to metal salts/sulfide mole ratio. Ratios used in preparation of these electroactive materials are presented in Table 1.

**Table 1.** Mole ratio of the metal salts and S<sup>2-</sup>

electrode	mole ratio		mole	
	(Cu <sup>2+</sup> ; Ag <sup>+</sup> ) : S <sup>2-</sup>		Cu <sup>2+</sup> ; Ag <sup>+</sup>	S <sup>2-</sup>
A	1 : 0.5		0.02; 0.04	0.02
B	1 : 1		0.02; 0.04	0.04
C	1 : 1.8		0.02; 0.04	0.072

## 2.3. Electrode fabrication

Membranes from prepared materials were pressed at 5000 kg cm<sup>-3</sup> and membrane thickness was 1 mm. Back contact together with mounting of the pellets onto brass sticks was made with conductive silver epoxy resin (SPI Supplies Division, West Chester, USA). After drying at 75° C for 4 hours, electrodes were finally sealed by epoxy resin. After epoxy resin was dried, electrode were abraded with fine emery paper and polished with alumina powder down to 0.05 μm and rinsed with distilled water.

## 2.4. XRD analysis

Phase composition was determined by X-Ray powder diffraction (XRD) using a Philips X'Pert Pro diffractometer from CuKα radiation (X-Ray tube PW 3373/00 Cu LFF DK119707 at a current of 40 mA and voltage of 45 kV) and X'celerator detector. Continuous scanning was made in the range 4° < 2Theta < 70°. The observed phases were identified by comparison of obtained data with those from JCPDS (2004) PDF2 database using Philips X'Pert HighScore software.

### 2.5. Spectrophotometric measurements

A stock solution of  $1 \times 10^{-2}$  M ethylenediamine (EN) (Kemika, Zagreb, Croatia) solution was prepared by dissolution of certain amount of EN in appropriate volume of water. Electrodes had been soaked in  $10 \text{ cm}^3$  of  $10^{-2}$  M solution of ethylenediamine for 2 hours, after absorption spectra of ethylenediamine solution were recorded between 200 and 600 nm.

Varian UV-visible Spectrophotometer-50 C was used for recording absorption spectra.

### 2.6. Potentiometric measurements

External reference electrode was double junction electrode (Mettler Toledo InLab 301 electrode). The potentiometric measurements were carried out by means of Mettler Toledo SevenEasy pH meter, which was connected to a computer. The potential build up across the membrane electrode was measured using the following electrochemical cell assembly: ISE | test solution | external reference electrode). Before potentiometric measurements, electrodes were not conditioned. The potential was recorded after addition of standard  $\text{Cu}^{2+}$  solution in magnetically stirred 0.1 M  $\text{KNO}_3$ . The investigated concentration range was from  $1.0 \times 10^{-8}$  M to  $2.8 \times 10^{-2}$  M. Detection limits were estimated according to IUPAC [19] from the cross point of the lines fitted to the linear segments of potential vs.  $\log a_i$  curve, where  $a_i$  denotes single ion activity of the primary ion.

### 2.7. Impedance measurements

The experiments were carried out using a standard three-electrode electrochemical cell. The counter electrode was a platinum electrode and the reference electrode was a saturated calomel electrode (SCE).

All measurements were carried out using a Solartron SI 1287 electrochemical interface and a Solartron SI 1255 frequency response analyzer connected with a personal computer. Impedance spectra were recorded in 0.1 M  $\text{KNO}_3$  solution, with addition of  $\text{Cu}^{2+}$ , at room temperature within the frequency range of 100 kHz–30 mHz using 10 mV rms sinusoidal perturbation. All measurements were performed at the open circuit potential ( $E_{\text{ocp}}$ ).

## 3. RESULTS AND DISCUSSION

### 3.1. Characterization of membrane material

The materials which were prepared by simultaneous precipitation of silver-copper sulfides has been analyzed by using X-ray diffraction at the polycrystalline materials. X-Ray diffraction patterns are shown at the Figure 1. Qualitative analyses of the different electrode materials were made by comparing experimental diffraction data with the diffraction data for known compounds stored in the JCPDS database. Results of analyses showed the presence of crystal phases  $\text{Ag}_{1.2}\text{Cu}_{0.8}\text{S}$  (PDF #12-

152),  $\text{Ag}_3\text{CuS}_2$  (Jalpaite, PDF #12-207),  $\text{AgCuS}$  (PDF #65-2499),  $\text{CuAgS}$  (Stromeyerite, PDF #79-1579) and  $\text{Ag}$  (PDF #04-0783).

The diffraction pattern of material denoted as electrode A (Fig.1) showed the difference toward electrode materials denoted as electrode B and C in the absence of the crystal phases  $\text{Ag}_3\text{CuS}_2$  (jalpaite) and clearly indicated a presence of the metallic silver. Also, small amount of the metallic silver, in the diffraction pattern of the electrode B, was observed.

In the diffraction pattern of the electrode material C, the determination of the metallic silver was hindered, due to the position of silver diffraction maximums, ( $2\theta$  38.13° and 64.45°), overlapped with  $\text{Ag}_3\text{CuS}_2$  jalpaite diffraction maximums. Also, third characteristic diffraction maximum for the metallic silver at the position  $2\theta$  at 44.29° was absent in the powder pattern.

The presence of the crystal phases  $\text{AgCuS}$  and  $\text{CuAgS}$  (Stromeyerite) was only observed in the material of electrode A, while crystal phase  $\text{Ag}_{1.2}\text{Cu}_{0.8}\text{S}$  was observed in the materials of electrode A and C.

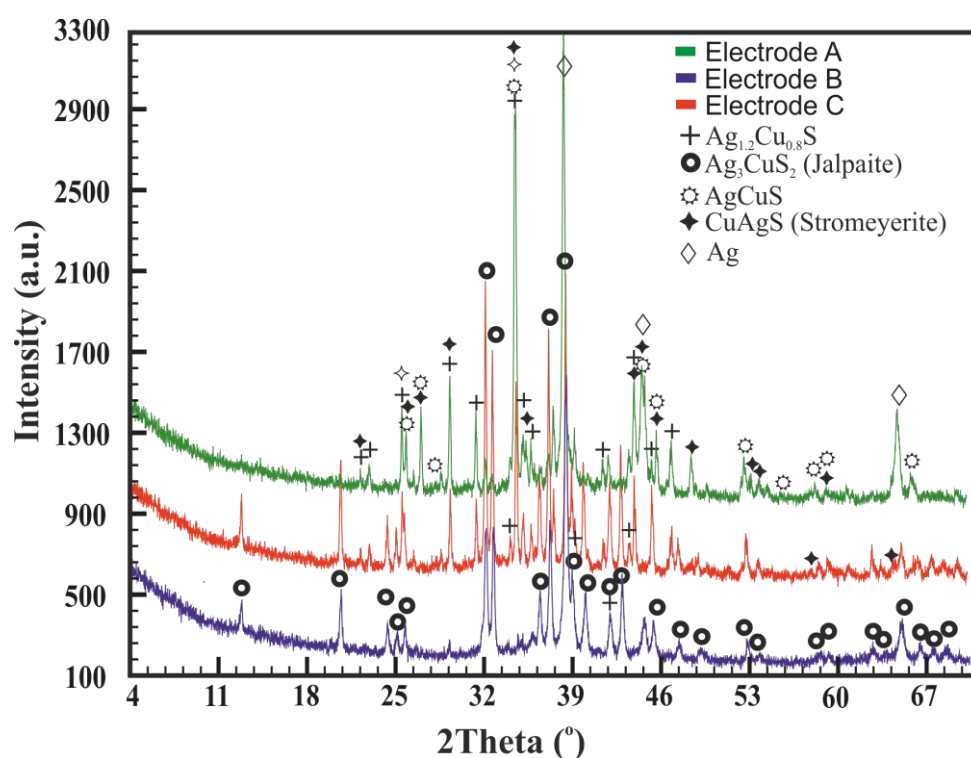


**Figure 1.** XRD pattern of prepared electroactive materials at different metal salts/sulfide mole ratio

### 3.2. Potentiometric behaviors of electrodes

To maintain a constant ionic strength, potentiometric measurements were performed in 0.1 M  $\text{KNO}_3$  at 25 °C with constant stirring, as it well known that different stirring rate have a effects on electrode surface adsorption, as also on diffusion rate [20]. Figure 2 shows the potentiometric responses of electrodes, with different compositions, toward  $\text{Cu}^{2+}$  at pH 4.5.

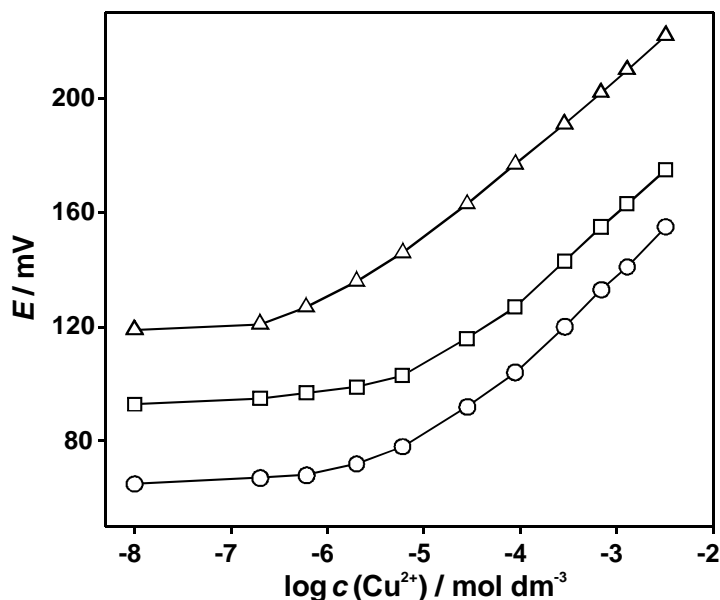


**Figure 2.** Calibration curves obtained by successive increasing of Cu<sup>2+</sup> concentration for: electrode A (○); electrode B (□); electrode C (△)

Response characteristic of electrodes are presented in Table 2. Near-Nernstian response, with slope with the slope of 28 mV per decade was observed C, while sub-Nernstian slope of 26.5 mV per decade was noticed for electrode B. Slope for electrode A was 32.5 mV per decade. Compared to electrode A and B, electrode C had extended linear range down to  $2.8 \times 10^{-7}$  M, with a detection limit of  $1.4 \times 10^{-7}$  M.

**Table 2.** The potentiometric characteristics of electrodes

electrode	ratio Me-salts : S <sup>2-</sup>	linear range (M)	detection limit (M)	slope (mV dec <sup>-1</sup> )
A	1 : 0.5	$5.8 \times 10^{-6}$ - $1.0 \times 10^{-2}$	$1.5 \times 10^{-6}$	32.5
B	1 : 1	$6.1 \times 10^{-6}$ - $1.0 \times 10^{-2}$	$2.5 \times 10^{-6}$	26.5
C	1 : 1.8	$2.8 \times 10^{-7}$ - $1.0 \times 10^{-2}$	$1.4 \times 10^{-7}$	28.0

Differences in detection limit can be attributed mainly to different solubility of electrode materials. To investigate a solubility of prepared materials, electrode had been soaked, in certain volume of  $10^{-2}$  solution of ethylenediamine (pH = 10.5), for 2 hours, after absorption spectra of ethylenediamine solution were recorded between 200 and 600 nm. Although longer wave lengths were expected due to dissolved copper [21] and Tomic [22] or even in infrared spectra due to silver-ethylenediamine complexes [23). However, absorption maximum was observed at 230 nm. This wavelength is expected when ethylenediamine is in large excess over a total copper concentration [24]. Thus, peak high is directly proportioned to concentration of copper complex in solution, which concentration is in dependence of Cu<sup>2+</sup>.

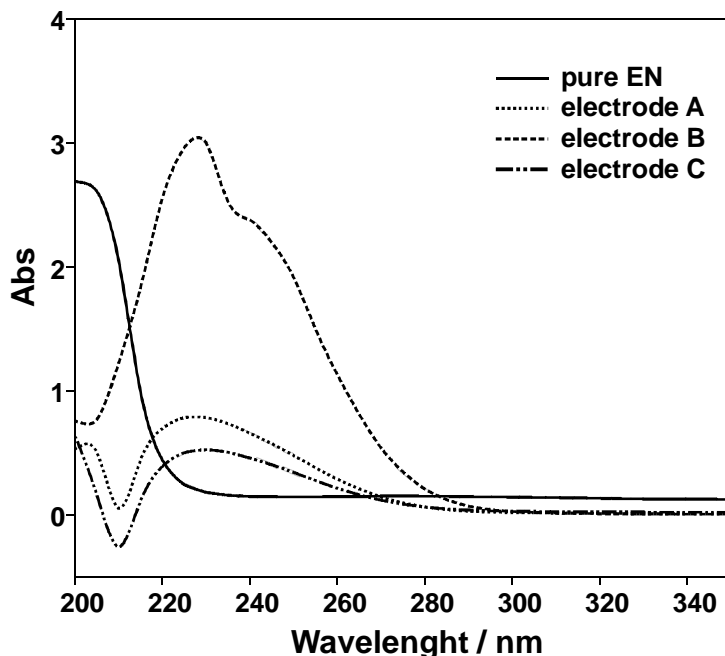


**Figure 3.** Absorption spectra of the EN solutions in which electrodes were been soaked for 2 hours.

According to above mentioned and from Figure 3, it was concluded that electrode solubility follows the pattern  $B > A > C$ . Surprisingly, standard potential of electrode did not follow this pattern (see Figure 2) as standard potential would be more positive at increased solubility. Dissolution of electrode is followed by oxidation of electrode to form sparingly soluble salt (viz.,  $\text{Cu}_3(\text{SO}_4)(\text{OH})_4$ ) or/and soluble  $\text{CuSO}_4$  [13] which alter the stoichiometry of the electrode surface and may cause a change in the standard electrode potential [25]. Also, formation of soluble salts is related to the high detection limits of electrode A and B as consequence of adsorption of  $\text{Cu}^{2+}$  onto membrane surface by equilibration with sparingly soluble salts. As electrode B is more soluble than A standard potential of electrode B is higher (due to adsorption).

### 3.3. Effect of pH

Effect of pH on the potential responses of membrane electrodes were determined at  $1.0 \times 10^{-4}$  M  $\text{Cu}^{2+}$  concentration. A pH range between 1 and 6 was controlled by using  $\text{HNO}_3$  solution. pH values above 6 did not considered as it is known that at higher pH (values above 6.5) hydrolysis of  $\text{Cu}^{2+}$  together with formation of a hydroxyl copper complexes would occur [26]. Widest range (between pH range 2.5 - 6) of constant potential versus pH was obtained with the electrode C, while potential remained constant over a pH range 3.2 - 6 and 4.5 - 6 for the electrodes A and B, respectively (see Figure 4). Narrowed pH range of the electrodes A and B indicates their higher solubility at pH values lower than 3.2 and 4.5, respectively compared to the electrode C. Also, wideness of pH range follows pattern ( $B < A < C$ ) which is in correlation with solubility pattern ( $B > A > C$ ). So, it can be concluded if electrode is more soluble (pattern  $B > A > C$ ), pH range of constant potential become more narrowed.

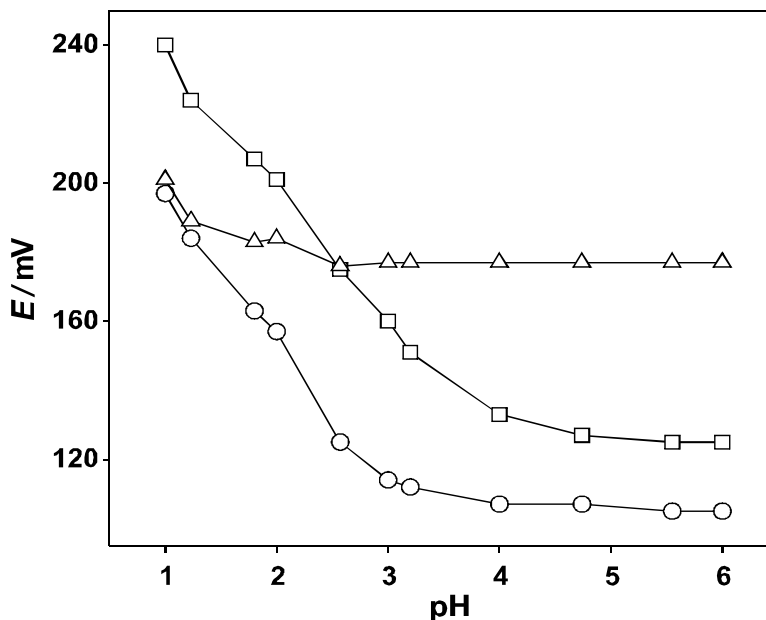


**Figure 4.** The effect of pH on the potentiometric response in  $1.0 \times 10^{-4}$  M of  $\text{Cu}^{2+}$  of the electrodes: A (○); B (□); C (△)

### 3.4. Time response

The response time of the electrodes was measured at 10-fold increase of the  $\text{Cu}^{2+}$  concentration with method proposed by IUPAC [19]. The response times were fast and same trend was observed for reverse process as well. All prepared electrodes gave the response time within 10 seconds in entire measurement range (see Figure 5).

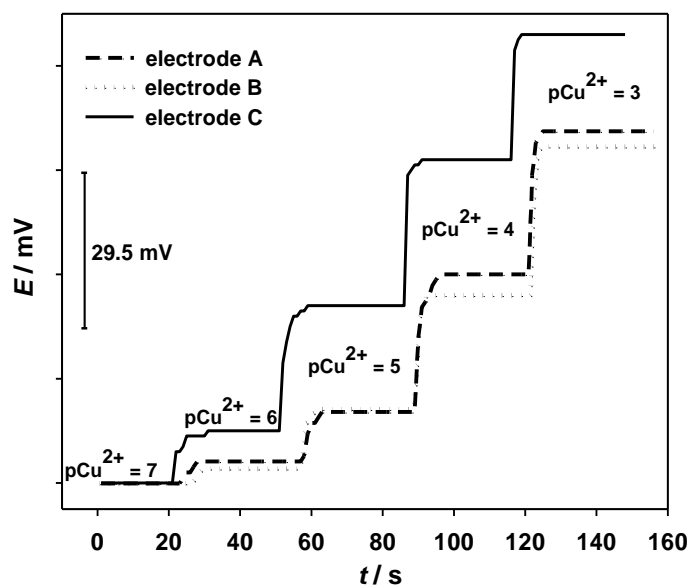


**Figure 5.** Dynamic response of electrodes on different concentration of  $\text{Cu}^{2+}$

3.5. EIS studies on of the electrodes

The Nyquist plots of three electrodes, at different  $\text{Cu}^{2+}$  concentration, are shown in Figure 6. The EIS spectra were fitted to the equivalent circuits shown in Figure 7. A constant phase element (CPE) is a modified capacitance and since the phase angle does not amount to  $-90^\circ$ , the electrode impedance may be precisely described by a constant-phase element (CPE):  $Z(\text{CPE}) = [Q(j\omega)^n]^{-1}$ , where  $Q$  is the constant,  $\omega$  is the angular frequency, and  $n$  is the CPE power. The  $n$  is an adjustable parameter that usually lies between 0.5 and 1, the ideal capacitor is described with  $n = 1$  [27].

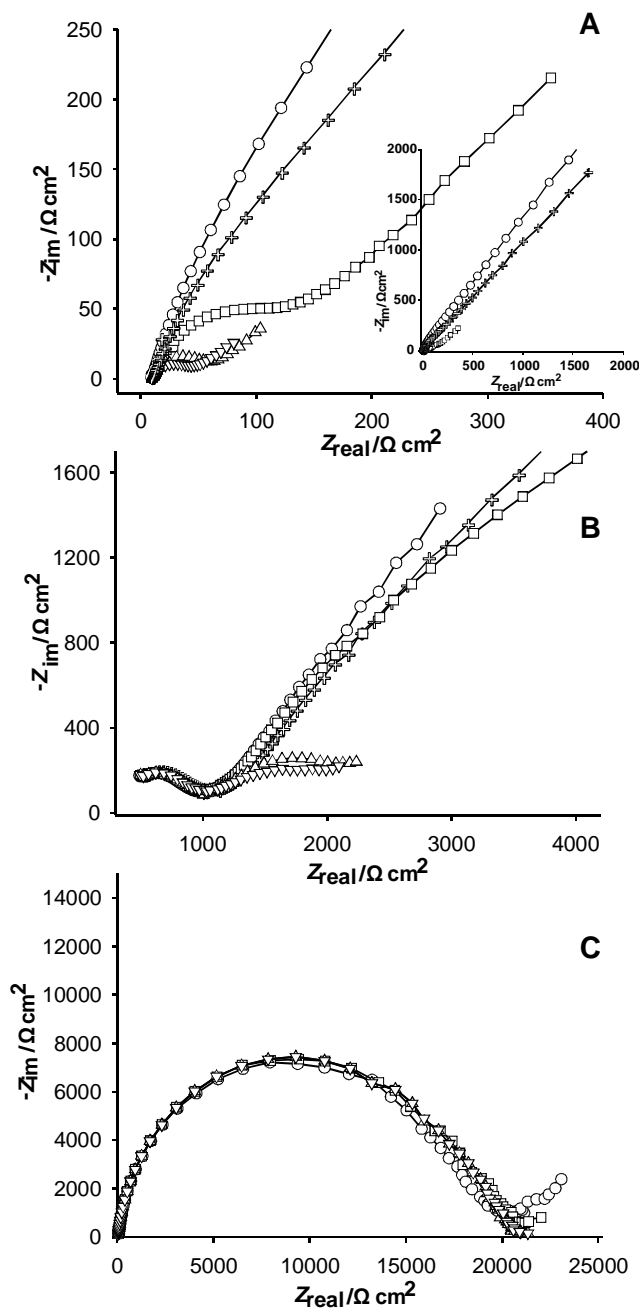


**Figure 6.** Impedance spectra, at obtained in: 0.1  $\text{KNO}_3$  ( $\circ$ ); 0.1  $\text{KNO}_3 + 10^{-5} \text{ M Cu}^{2+}$  ( $\square$ ); 0.1  $\text{KNO}_3 + 10^{-3} \text{ M Cu}^{2+}$  ( $\triangle$ ); 0.1  $\text{KNO}_3 + 10^{-2} \text{ M Cu}^{2+}$  ( $\nabla$ ); 0.1  $\text{KNO}_3$  immediately after measurement in  $10^{-2} \text{ M Cu}^{2+}$  ( $\oplus$ ), for electrodes A , B, C

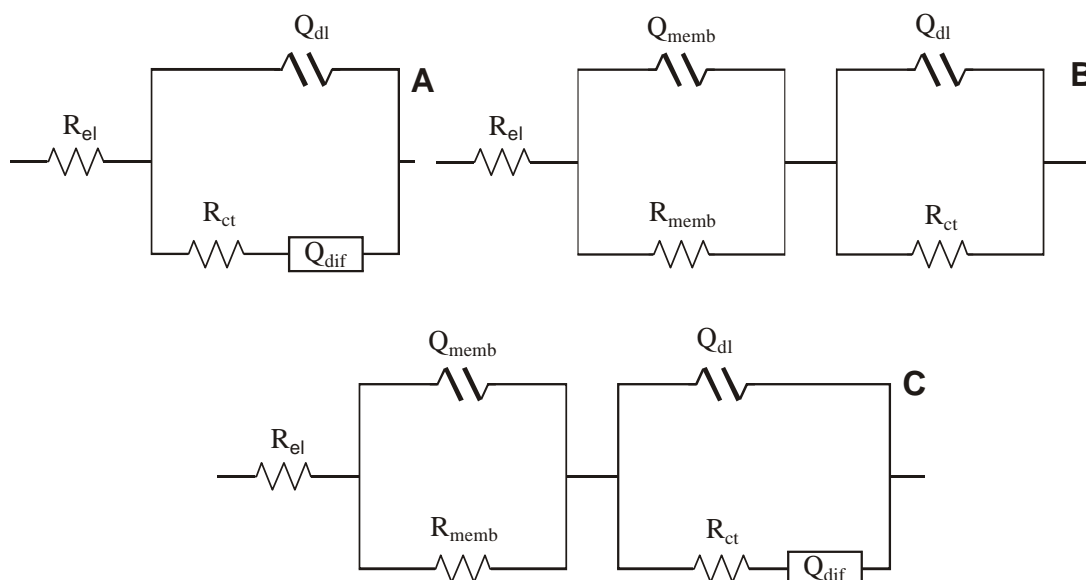


**Figure 7.** Equivalent electrical circuit models used for analysis

**Table 3.** Impedance parameters for electrode C, at different concentration of Cu<sup>2+</sup>, as determinate using the equivalent circuit presented in Fig. 7 (models C)

pCu <sup>2+</sup>	R <sub>el</sub> (Ω cm <sup>2</sup> )	R <sub>memb</sub> (Ω cm <sup>2</sup> )	Q <sub>memb</sub> × 10 <sup>-6</sup> (Ω <sup>-1</sup> s <sup>n</sup> cm <sup>-2</sup> )	n	R <sub>ct</sub> (Ω cm <sup>2</sup> )	Q <sub>dl</sub> × 10 <sup>-6</sup> (Ω <sup>-1</sup> s <sup>n</sup> cm <sup>-2</sup> )	n	Q <sub>dif</sub> × 10 <sup>-6</sup> (Ω <sup>-1</sup> s <sup>n</sup> cm <sup>-2</sup> )	n
no Cu <sup>2+</sup>	30	11546	0.036	0.94	7377	0.68	0.76	296	0.30
5	30	12686	0.037	0.94	7455	0.96	0.75	766	0.30
3	23	12290	0.036	0.95	8699	0.96	0.73	-	-
2	23	13105	0.037	0.94	7456	1.44	0.71	-	-

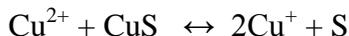
**Table 4.** Impedance parameters for electrode B, at different concentration of Cu<sup>2+</sup>, as determinate using the equivalent circuits presented in Fig. 7 (models B)

pCu <sup>2+</sup>	R <sub>el</sub> (Ω cm <sup>2</sup> )	R <sub>memb</sub> (Ω cm <sup>2</sup> )	Q <sub>memb</sub> × 10 <sup>-6</sup> (Ω <sup>-1</sup> s <sup>n</sup> cm <sup>-2</sup> )	n	R <sub>ct</sub> (Ω cm <sup>2</sup> )	Q <sub>dl</sub> × 10 <sup>-6</sup> (Ω <sup>-1</sup> s <sup>n</sup> cm <sup>-2</sup> )	n
no Cu <sup>2+</sup>	250	783	1.9	0.55	51124	616	0.42
5	282	704	1.12	0.60	19161	604	0.47
3	256	697	0.98	0.60	1679	505	0.36
2	246	676	0.92	0.60	1688	596	0.30
no Cu <sup>2+*</sup>	305	732	1.15	0.60	48000	669	0.36

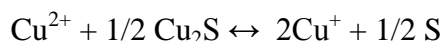
\* Electrode was taking out from solution and washed in distilled water and slightly wiped with paper, after impedance spectra was recorded in 0.1 M KNO<sub>3</sub> solution.

The impedance spectra for electrode C recorded with and without presence of Cu<sup>2+</sup>, which showed two time constants, were fitted to the equivalent circuit presented at Figure 7 C and results of fitting are summarized in Table 3. From Figure 6 and from results of fitting summarized in Table 3 it is obvious that increasing of Cu<sup>2+</sup> concentration did not influenced on the high frequency time constant,

which is proposed to be a result of bulk properties of the membrane (i.e. membrane resistance  $R_{\text{memb}}$  and its geometric capacitance  $Q_{\text{memb}}$ ). Second time constant is related to the charge-transfer resistance ( $R_{\text{ct}}$ ) in parallel with double layer capacitance ( $Q_{\text{dl}}$ ) for the reactions that describe potentiometric response which were proposed by Westall [28] and Hulanicki [29].



or



Values of charge transfer resistance ( $R_{\text{ct}}$ ) and double layer capacitance ( $Q_{\text{dl}}$ ) remained constant over measured concentration range, indicating that a charge transfer is low rate process and mainly independent of diffusion. Although, negligible contribution of diffusion can be observed only at concentration lower than  $10^{-5}$  M, the inclusion of small Warburg impedance term in the equivalent circuit was needed to obtain a good correlation between fitted and experimental data (model presented at Figure 7 C). Diminishing of diffusion impedance was noticed at elevated  $\text{Cu}^{2+}$  concentrations, as it can be seen at Figure 6. As impedance spectra were independent of  $\text{Cu}^{2+}$  concentrations, Nernstian response was observed at measured concentration range, since there is no  $\text{Cu}^{2+}$  perturbation in diffusion layer and concentration profile of the  $\text{Cu}^{2+}$  from electrode surface toward bulk of the solution was formed immediately.

Impedance spectra for electrode B, recorded at different  $\text{Cu}^{2+}$  concentration, are presented at Figure 6 and results of fitting to the equivalent electric circuits (Figure 7 B) are summarized in Table 4. The spectrum recorded with no presence of  $\text{Cu}^{2+}$  reveals a time constant in the high frequency region which can be attributed to the bulk properties of membrane i.e. membrane resistance ( $R_{\text{memb}}$ ) and geometric capacitance of the membrane ( $Q_{\text{memb}}$ ). Difference in bulk resistances of the electrode B and C can be attributed to small amount of the metallic silver in electrode B formed in the precipitation process. By addition of  $\text{Cu}^{2+}$ , second time constant become discernible and it can be attributed to the charge transfer process, according proposed mechanism. However, as results of the fast and high rate of the charge transfer process and from values of the  $n$  in  $Q_{\text{dl}}$ , it can be seen a strong influence of the diffusion thus making center of second semicircle more depressed. Bearing on mind discussion for electrode C, diffusion of the  $\text{Cu}^{2+}$  in the case of electrode B become limiting factor concerning Nernstian response since constant concentration profile was not achieved.

Impedance spectra obtained for electrode A, at different  $\text{Cu}^{2+}$  concentration, are presented in Figure 6A. The data were fitted with the equivalent circuit, shown in Figure 7 A and the results of fitting procedure are given in Table 5. As it can be seen, impedance spectra are characterized with only one time constant that described interfacial process at the membrane/solution interface, according proposed mechanism. It must be emphasis that this electrode did not showed electrical resistance, which is not surprising, as the membrane material of this electrode contains certain amount of the metallic silver (higher than for electrode B), as it described in the Chapter 3.1.  $R_{\text{ct}}$  is strongly dependent on the  $\text{Cu}^{2+}$  concentration in the solution. Its decrease by increasing  $\text{Cu}^{2+}$  concentration, indicates that the kinetics of the charge transfer is favored for an elevated  $\text{Cu}^{2+}$  concentration.

Warburg-like diffusion element ( $Q_{dif}$ ), at the low frequency region, must be related to diffusion of  $Cu^{2+}$  and have same influence as it described for electrode B.

**Table 5.** Impedance parameters for electrode A, at different concentration of  $Cu^{2+}$ , as determinate using the equivalent circuit presented in Fig. 7 A

$pCu^{2+}$	Rel ( $\Omega\text{ cm}^2$ )	Rct ( $\Omega\text{ cm}^2$ )	$Q_{dl} \times 10^{-6}$ ( $\Omega^{-1}\text{ s}^n\text{ cm}^{-2}$ )	n	$Q_{dif} \times 10^{-6}$ ( $\Omega^{-1}\text{ s}^n\text{ cm}^{-2}$ )	n
no $Cu^{2+}$	10	686	211	0.78	339	0.53
5	10	121	230	0.75	5522	0.47
4	10	47	369	0.70	26891	0.40
3	10	31	443	0.70	30845	0.35
no $Cu^{2+}$ *	10	301	230	0.77	644	0.50

\* Electrode was taking out from solution and washed in distilled water and slightly wiped with paper, after impedance spectra was recorded in 0.1 M  $KNO_3$  solution.

It must be emphasis that impedance measurements were performed with addition of  $Cu^{2+}$  into solution without taking out electrode. When electrodes were take out from solution and washed in distilled water, impedance spectra in fresh  $KNO_3$  solution without  $Cu^{2+}$  were recorded (see Figure 6). Impedance spectra for electrodes A and B were not identical as those recorded when electrodes were "freshly" prepared (before any contact with  $Cu^{2+}$  ions). It can be results of the adsorbed  $Cu^{2+}$  in the pore of the electrode surface (since electrode surface is modified by dissolution) and its releasing in the pure  $KNO_3$ . Interesting, this hysteresis effect become more apparent as electrode is more soluble and it follow solubility pattern ( $B > A > C$ ) which is same as detection limit pattern. This is in accordance to the results obtained with spectrophotometric and potentiometric measurements. For electrode C this effect is mostly negligible. Such behavior can explain differences in the detection limit between electrodes (see Table 2). When this film was removed by abrading or polishing, impedance spectra was identical to initial spectra (results are not showed).

#### 4. CONCLUSION

X-ray diffraction at the three different materials, prepared by co-precipitation of the mixed metals ions ( $Cu^{2+}$ ,  $Ag^+$ ) and  $S^{2-}$  (from  $Na_2S$ ) at different mole ratio, showed presence of different ternary compounds.  $Ag_3CuS_2$  was founded in materials prepared in excess of sulfide together with metallic silver (electrode B) and  $Ag_{1.2}Cu_{0.8}S$  (electrode C). XRD pattern of material prepared in the excess of the metallic ions did not revealed presence of  $Ag_3CuS_2$  but  $Ag_{1.2}Cu_{0.8}S$  and  $CuAgS$  and  $Ag$ .

Differences in the electrical conductivity can be attributed to the presence of the metallic silver which is confirmed by XRD measurements. EIS measurement revealed different resistance of the electrodes as follows: no resistance for electrode A; around 700  $\Omega$  for electrode B; around 12 000  $\Omega$

for electrode C. The presence of the metallic silver is attributed to the different mole ratio of metal salts and sulfide used in preparation of the electroactive materials.

Differences in detection limits correlates to the different solubility of electrode materials which follows pattern (B>A>C). Associated to the solubility, hysteresis effect was observed and its extent follows solubility and detection limit patterns, which was proved by EIS measurement. This effect is attributed to the adsorption of the  $\text{Cu}^{2+}$  in the pore of the electrode surface, modified due to electrode dissolution. Negligible hysteresis effect was noticed for electrode C.

Impedance measurements revealed that a lack of the Nernstian response can be attributed to the perturbation in diffusion layer associated with high rate of the charge transfer process at the electrode/solution surface, causing concentration profile of  $\text{Cu}^{2+}$  in diffusion layer inconstant. Nernstian response was observed for electrode C, which impedance spectra were mainly independent of  $\text{Cu}^{2+}$  concentration.

Decrease of the electrode materials resistance results in strongly dependence of the charge transfer resistance ( $R_{ct}$ ) on the  $\text{Cu}^{2+}$  concentration, indicating that the kinetics of the charge transfer process is favored for an elevated  $\text{Cu}^{2+}$  concentration. By increasing electrical resistance of the electrode (see electrode C), charge transfer become low rate process and mainly independent of diffusion, causing that concentration profile of the  $\text{Cu}^{2+}$  is formed immediately and as consequence Nernstian response can be observed.

## References

1. G. J. M Heijne, W. E. van der Linden, G. den Boef, *Anal. Chim. Acta*, 89 (1977) 287
2. G. J. M Heijne, W. E. van der Linden, *Anal. Chim. Acta*, 93 (1977) 99
3. R. Tomova, G. Spasov, R. Stoycheva-Topalova, A. Buroff, *Sens. Actuators B-Chemical*, 103 (2004) 277
4. S. P. Awasthi, N. S. Shenoy, T. P. Radhakrishnan, *Analyst*, 119 (1994) 1361
5. M. T. Neshkova, A. A. Kirkova, R. W. Cattrall, C. G. Gregorio, A. M. Bond, *Anal. Chim. Acta* 362 (1998) 221
6. M. Buzuk, S. Brinić, E. Generalić, M. Bralić, *Croatica Chemica Acta*, 82 (2009) 801
7. S. Brinić, M. Buzuk, E. Generalić, M. Bralić, *Acta chimica Slovenica*, 57 (2010) ; 318
8. S. Brinić, M. Buzuk, M. Bralić, E. Generalić, *Journal of Solid State Electrochemistry*, 16 (2012) 1333
9. L. P. Singh, J. M. Bhatnagar, *Talanta*, 64 (2001) 313
10. A. Abbaspour, M. A. Kamyabi, *Anal. Chim. Acta*, 455 (2002) 225
11. M. M. Ardakani, S. H. Mirhoseini, M. Salvati-Niasari, *Acta Chim. Slov.*, 53 (2006) 197
12. J. Gulens, *Selective electrode Rev.*, 9 (1987) 127
13. R. De Marco, *Anal. Chem.*, 66 (1994) 3202
14. A. Zirino, R. de Marco, I. Rivera, B. Pejcic, *Electroanalysis*, 14 (2002) 493
15. M. G van der Berg, *Marine Chemistry*, 71 (2000) 331
16. A. Lewenstam, T. Sokalski, A. Hulanicki, *Talanta*, 32 (1985) 531
17. R. De Marco, R. Eriksen, A. Zirino; *Anal. Chem.*, 70 (1998) 4683
18. J. D. Czaban, G. A. Rechnitz, *Anal. Chem.*, 45 (1973) 471
19. R. P. Buck, E. Lindner, *Pure & Appl Chem*, 66 (1994) 2527
20. A. Zirino et al., *Marine Chemistry*, 61 (1998) 173
21. H. B. Jonassen, T. H. Dexter, *J. Am. Chem. Society*, 71 (1949) 1553

22. E. A. Tomic, J. A. Bernard, *Anal. Chem.*, 34 (1962) 632
23. G. Newman; D.P. Powell, *J. Chem. Soc.*, (1962) 3447
24. H. Hauser, E. J. Billo, D. W. Margerum, *Journal of American Chemical Society*, 93 (1971) 4173
25. M. Koebel, *Anal. Chem.*, 46 (1974) 1559
26. L. Hidmi, M. Edwards, *Envir. Sci. Technol.*, 33 (1999) 2607
27. M. Bralić et. al, *Talanta*, 55 (2001) 581
28. J. C. Westall, F. M. M. Morel and D. N. Hume, *Anal. Chem.*, 51 (1979) 1792
29. A. Hulanicki, A. Lewenstam, *Talanta*, 23 (1976) 661